Shell evolution beyond $N = 40$: ^{69,71,73}Cu

E. Sahin,[1,2] M. Doncel,[3,4] K. Sieja,[5] G. de Angelis,[1] A. Gadea,[6] B. Quintana,[3] A. Görgen,[2,7] V. Modamio,[1] D. Mengoni,[8,9,10] J. J. Valiente-Dobón,[1] P. R. John,[10] M. Albers,[11] D. Bazzacco,[10] G. Benzoni,[12] B. Birkenbach,[11] B. Cederwall,[4] E. Clément,[13] D. Curien,[5] L. Corradi,[1] P. Désesquelles,[14] A. Dewald,[11] F. Didierjean,[15,16] G. Duchêne,[15,16] J. Eberth,[11] M. N. Erduran,[17] E. Farnea,[10,*] E. Fioretto,[1] G. de France,[13] C. Fransen,[11] R. Gernhäuser,[18] A. Gottardo,[1,10,†] M. Hackstein,[11] T. Hagen,[2] A. Hernández-Prieto,[3] H. Hess,[11] T. Hüyük,[6] A. Jungclaus,[19] S. Klupp,[18] W. Korten,[7] A. Kusoglu,[20] S. M. Lenzi,[10] J. Ljungvall,[7,14] C. Louchart,[7,‡] S. Lunardi,[9,10] R. Menegazzo,[10] C. Michelagnoli,[10,§] T. Mijatović,[21] B. Million,[12] P. Molini,[9,10] G. Montagnoli,[10] D. Montanari,[1] O. Möller,[22] D. R. Napoli,[1] A. Obertelli,[7] R. Orlandi,[19,23] G. Pollarolo,[24] A. Pullia,[12,25] F. Recchia,[10] P. Reiter,[11] D. Rosso,[1] W. Rother,[11] M.-D. Salsac,[7] F. Scarlassara,[10] M. Schlarb,[18] S. Siem,[2] Pushpendra P. Singh,[1,‖] P.-A. Söderström,[26,¶] A. M. Stefanini,[1] O. Stézowski,[27] B. Sulignano,[7] S. Szilner,[21] Ch. Theisen,[7] C. A. Ur,[10] and M. Yalcinkaya[20]

[1]*Istituto Nazionale di Fisica Nucleare, Laboratori Nazionali di Legnaro, 35020 Legnaro, Italy*
[2]*Department of Physics, University of Oslo, P.O. Box 1048, Blindern, N-0316 Oslo, Norway*
[3]*Laboratorio de Radiaciones Ionizantes, University of Salamanca, Spain*
[4]*Department of Physics, Royal Institute of Technology, SE-10691 Stockholm, Sweden*
[5]*Institute Pluridisciplinaire Hubert Curien, 23 rue du Loess, F-67037 Strasbourg Cedex 2, France*
[6]*IFIC, CSIC, València, Spain*
[7]*Institut de Recherche sur les lois Fondamentales de l'Univers–IRFU, CEA/DSM, Centre CEA de Saclay, F-91191 Gif-sur-Yvette Cedex, France*
[8]*Nuclear Physics Research Group, University of the West of Scotland, High Street, Paisley, PA1 2BE, Scotland, United Kingdom*
[9]*INFN Sezione di Padova, I-35131 Padova, Italy*
[10]*Dipartimento di Fisica e Astronomia dell'Università di Padova, I-35131 Padova, Italy*
[11]*Institut für Kernphysik, Universität zu Köln, Zülpicher Strasse 77, D-50937 Köln, Germany*
[12]*INFN Sezione di Milano, I-20133 Milano, Italy*
[13]*GANIL, CEA/DSM-CNRS/IN2P3, F-14076 Caen Cedex 05, France*
[14]*Centre de Spectrométrie Nucléaire et de Spectrométrie de Masse–CSNSM, CNRS/IN2P3, and Université Paris-Sud, F-91405 Orsay campus, France*
[15]*Université de Strasbourg, IPHC, 23 rue du Loess, 67037 Strasbourg, France*
[16]*CNRS, UMR7178, 67037 Strasbourg, France*
[17]*Faculty of Engineering and Natural Sciences, Istanbul Sabahattin Zaim University, Istanbul, Turkey*
[18]*Technische Universität München, Germany*
[19]*Instituto de Estructura de la Materia, CSIC, Madrid, E-28006 Madrid, Spain*
[20]*Department of Physics, Faculty of Science, Istanbul University, Vezneciler/Fatih, 34134, Istanbul, Turkey*
[21]*Ruđer Bošković Institute, Zagreb, Croatia*
[22]*Institut für Kernphysik, Technische Universität Darmstadt, Darmstadt, Germany*
[23]*ASRC, JAEA, Tokai, Ibaraki, Japan*
[24]*Dipartimento di Fisica Teoria, Università di Torino, Italy*
[25]*Dipartimento di Fisica, Università di Milano, I-20133 Milano, Italy*
[26]*Department of Physics and Astronomy, Uppsala University, SE-75120 Uppsala, Sweden*
[27]*Université de Lyon, CNRS-IN2P3, Institut de Physique Nucléaire de Lyon, Villeurbanne, France*

(Received 19 December 2014; revised manuscript received 6 February 2015; published 2 March 2015)

The level structure of the neutron-rich ^{69}Cu, ^{71}Cu, and ^{73}Cu isotopes has been investigated by means of multinucleon transfer reactions. The experiment was performed at Laboratori Nazionali di Legnaro using the AGATA Demonstrator array coupled to the PRISMA magnetic spectrometer. Lifetimes of excited states in Cu nuclei were measured with the recoil-distance Doppler-shift method. The resulting electromagnetic matrix elements for transitions from excited states in ^{69,71,73}Cu nuclei are used to assess the collective or single-particle character of these states. The results are compared with predictions of large-scale shell-model calculations, giving further insight into the evolution of the proton pf shell as neutrons fill the $1g_{9/2}$ orbital.

DOI: 10.1103/PhysRevC.91.034302 PACS number(s): 21.10.Tg, 21.60.Cs, 23.20.Lv

[*]Deceased
[†]Present address: Institut de Physique Nucléaire, CNRS/IN2P3, and Université Paris Sud, Orsay, 91406, France.
[‡]Present address: Institut für Kernphysik, Technische Universität Darmstadt, Darmstadt, Germany.
[§]Present address: GANIL, CEA/DSM-CNRS/IN2P3, F-14076 Caen Cedex 05, France.
[‖]Present address: Department of Physics, Indian Institute of Technology Ropar, Rupnagar, Punjab 140001, India.

I. INTRODUCTION

Current nuclear structure studies are paying considerable attention to the search for anomalies in the shell structure of nuclei with large neutron-to-proton ratios. In these exotic regions of the nuclear chart, the separation between single-particle orbitals can be altered due to a changing ratio between $T = 1$ and $T = 0$ components of the nuclear force. As a consequence, energy gaps between single-particle orbitals can be reduced and new shell gaps may appear, altering the magic numbers that were first explained by Goeppert-Mayer in 1948 [1]. The interplay among central, spin-orbit, and tensor components of the effective nucleon-nucleon interaction can shift effective single-particle energies relative to each other as protons and neutrons fill certain orbitals near the Fermi surface in nuclei with large neutron excess [2–11]. This shell evolution far from stability has been experimentally observed in different mass regions: The magic numbers at $N = 20$ and 28 disappear for very proton deficient nuclei, and new magic numbers at $N = 14$, 16, 32, and 34 seem to appear [12–18,18–23].

Shell-model calculations predict changes in the shell structure also for exotic nuclei near the $Z = 28$ and $N = 40$ and 50 shell closures [4–6,24–26]. The evolution of proton single-particle states as a function of neutron number for the chain of Ni isotopes between ^{68}Ni and ^{78}Ni was investigated using the GXPF1 residual interaction [4,5]. With increasing number of neutrons in the $\nu 1g_{9/2}$ orbital the energies of the proton effective single-particle states (ESPSs) are modified and lead to the inversion of the $\pi 2p_{3/2}$ and $\pi 1f_{5/2}$ orbitals. Furthermore, the $Z = 28$ shell gap was predicted to decrease as a result of the attraction between the $\pi 1f_{5/2}$ and the $\nu 1g_{9/2}$ orbitals and the repulsion between the $\pi 1f_{7/2}$ and $\nu 1g_{9/2}$ orbitals. A similar reduction in relative excitation energy between the $\pi 1f_{5/2}$ and $\pi 1f_{7/2}$ proton ESPSs has also been predicted using the new Gogny-type mean-field interaction GT2 in which the tensor interaction is implemented explicitly [27].

Neutron-rich Cu isotopes, having one proton outside the $Z = 28$ shell, are good probes of the single-particle structure in the ^{78}Ni region. Coulomb excitation and β-decay studies have provided detailed information on the excited states of the neutron-rich Cu isotopes up to $A = 73$ [28–31]. Several candidates were identified in these studies for states of mainly single-particle character based on the $\pi 1f_{5/2}$, $\pi 1f_{7/2}$, and $\pi 2p_{1/2}$ orbitals. Shell-model calculations including the effect of the tensor force predicted a lowering of the $\pi 1f_{5/2}$ orbital, which eventually crosses the $\pi 2p_{3/2}$ orbital and leads to a $5/2^-$ ground state in ^{75}Cu and the heavier odd-mass isotopes [24]. This inversion was confirmed by measurements of the ground-state spin and magnetic moment, which identified the ground state of ^{75}Cu as $5/2^-$ [32]. However, the level structure of the odd-mass, neutron-rich Cu isotopes is more complicated, and not only proton single-particle states but also core-coupled and collective states are expected to lie at low excitation energies. As an example, the first excited $9/2^+$ state in ^{65,67}Cu has been recently interpreted to be a core-coupled state involving the 3^- octupole phonon of the ^{64,66}Ni core when comparing the experimental $B(E3)$ strength of the $9/2^+$ state to the particle-phonon calculations [33,34]. The intrinsic nature of the negative-parity states can be unveiled by measuring the reduced quadrupole transition probability $B(E2)$ for transitions de-exciting those states and comparing them with states of the neighboring even-even $(A-1)$ Ni nuclei and with shell-model calculations. The single-particle nature of the $5/2^-$ state for the odd-mass $^{67-73}$Cu isotopes was confirmed by means of Coulomb excitation studies [30]. In the same work, by measuring $B(E2)$ values, the $1/2^-$ states were identified and characterized as low-lying collective states, while the $7/2^-$ states were interpreted as particle-core excitations, based on the similarity of the $B(E2)$ values with the respective $(A-1)$ Ni neighbors [30].

According to calculations based on the particle-core coupling model (PCM) [35], the low-lying $7/2^-$ states appearing in Cu nuclei can be explained either as two-particle–one-hole (2p-1h)$(\pi 2p_{3/2})^2 (\pi 1f_{7/2})^{-1}$ states or core-coupled states with $\pi 2p_{3/2} \otimes 2_1^+ (^{A-1}\mathrm{Ni})$ configuration. Note that 2p-1h proton excitations in the neutron-rich Cu isotopes give information on the energy difference between the proton $1f_{7/2}$ and $1f_{5/2}$ orbitals and that they are hence sensitive to the size of the shell gap at $Z = 28$, as $N = 50$ is approached. Recent large-scale shell-model (LSSM) calculations with an empirically adjusted interaction have predicted the excitation spectrum in odd-mass Cu isotopes between $N = 40$ and $N = 50$, and the significance of proton-core excitations for the stability of the shell closure was extensively discussed [25,26]. Based on existing experimental data and the predictions of the LSSM calculations for Cu nuclei with increasing number of neutrons in the $1g_{9/2}$ orbital, the following configurations could give rise to $7/2^-$ states:

(i) the coupling of the $\pi 2p_{3/2}$ single-particle configuration to the 2_1^+ core excitation in the neighboring Ni isotope: $\pi 2p_{3/2} \otimes 2_1^+ (^{A-1}\mathrm{Ni})$,
(ii) the coupling of the $\pi 1f_{5/2}$ single-particle configuration to the 2_1^+ core excitation in the neighboring Ni isotope: $\pi 1f_{5/2} \otimes 2_1^+ (^{A-1}\mathrm{Ni})$, and
(iii) the 2p-1h excitation with one particle promoted from the $\pi 1f_{7/2}$ to the $\pi 2p_{3/2}$ orbital: $(\pi 2p_{3/2})^2 (\pi 1f_{7/2})^{-1}$.

The aim of the present work is to study the collective or single-particle character of the $7/2^-$ states deduced from the $B(E2)$ values. The characterization of these states and, in particular, the identification of the $(\pi 2p_{3/2})^2 (\pi 1f_{7/2})^{-1}$ particle-hole excitation across the $Z = 28$ shell gap will provide essential information on the size of the shell gap and, therefore, on the evolution of the shell structure close to ^{78}Ni.

II. EXPERIMENT AND METHODS

Neutron-rich Cu isotopes were populated via multinucleon transfer reactions using a ^{76}Ge beam and a thin, metallic ^{238}U target. The ^{76}Ge projectiles were accelerated to an energy of 577 MeV by the Tandem-XTU and the ALPI superconducting LINAC accelerators at Laboratori Nazionali di Legnaro (LNL), Italy. The target consisted of a 1.5 mg/cm^2 thick layer of ^{238}U

[¶]Present address: RIKEN Nishina Center, 2-1 Hirosawa, Wako, 351-0198 Saitama, Japan.

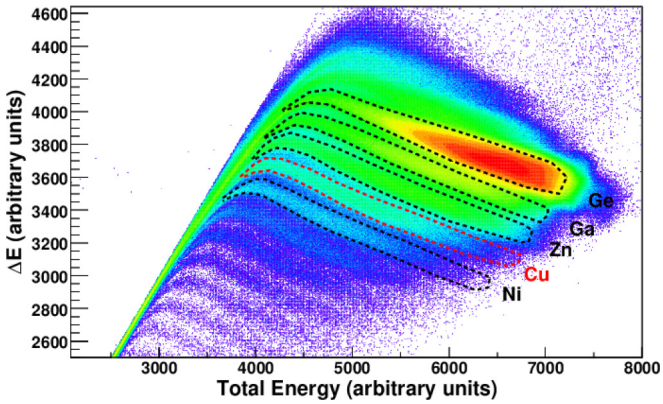

FIG. 1. (Color online) Energy loss ΔE versus total energy E of the ions detected at the PRISMA focal plane for the ^{76}Ge + ^{238}U reaction. The elements corresponding to the different proton stripping channels are indicated.

evaporated onto a ^{181}Ta backing of 1.4 mg/cm ^{2} thickness which was facing the beam. The Ta backing was necessary for stretching the target foil to obtain an even and smooth surface. The target was mounted at a variable distance from a ^{93}Nb degrader foil of 4.2 mg/cm ^{2} thickness in a compact plunger device from the University of Köln. Data were taken using the AGATA Demonstrator array [36,37] coupled to the PRISMA magnetic spectrometer [38]. The projectile-like reaction products were detected by the PRISMA spectrometer, which was placed at the grazing angle of 55° with respect to the beam direction. Element identification of the reaction products ranging from Ge to Ni isotopes was obtained by measuring the total energy and the characteristic energy loss of the ions arriving at the end of the focal plane of PRISMA. The ΔE-E identification matrix is shown in Fig. 1. The time of flight (TOF) between the large-area microchannel plate (MCP) entrance detector of PRISMA [39] and the multiwire parallel-plate avalanche counters (MW-PPAC) of its focal plane [40] was used to measure the absolute velocity and the mass of the ions. The average mass resolution achieved in the experiment was $\Delta A/A \approx 1/220$, allowing a very clean mass identification of all detected reaction products.

The γ rays following the de-excitation of the reaction products were detected by the AGATA Demonstrator array, placed at a distance of 18 cm from the target position and covering an angular range from 135° to 175° with respect to the spectrometer axis of PRISMA. The Doppler correction of the γ rays was performed on an event-by-event basis, taking the information of the recoil velocity vector determined by PRISMA and the angle between the velocity vector and the direction of the γ ray emitted from the recoil. At the time of the experiment, the AGATA Demonstrator consisted of four triple clusters, and its total-absorption efficiency was measured to be $\epsilon = 3.2\%$ at an energy of 1.332 MeV [41]. One AGATA triple cluster (ATC) detector consists of three HPGe crystals. Each crystal is 36-fold segmented to determine the position of individual interactions of the γ rays in the detector. The total charge deposited in each crystal is collected at the central core contact. Data from the AGATA Demonstrator array was processed on-line, and a pulse-shape analysis (PSA) algorithm based on a grid search [42] was applied to identify the position of the interaction points. A position resolution of better than 5 mm was achieved in the PSA procedure. High precision for the position resolution is crucial for the subsequent application of the γ-ray tracking algorithm [43,44], which reconstructs the energies of individual γ rays from the energies deposited at the interaction points. γ-ray events detected in the AGATA Demonstrator were correlated with ions detected at the focal plane of PRISMA through time stamping. The analysis of AGATA-PRISMA coincidences permitted us to identify the γ rays originating from the nuclei of interest and resulted in a significant suppression of unwanted background.

Lifetimes of excited states in Cu nuclei were measured using the differential recoil distance Doppler-shift (RDDS) method [45–48] with a plunger device that was designed for the coupling of the AGATA Demonstrator and the PRISMA spectrometer at LNL. In this variant of the RDDS method the velocity of the recoiling ions is reduced when they pass through a degrader foil that is mounted at micrometer distances from the target. The Doppler shift of a γ ray then depends on whether it was emitted before or after the recoil passed through the degrader. If the lifetime of the state of interest is of the same order of magnitude as the flight time between the target and degrader foils, γ rays from this state are observed with two components corresponding to different Doppler shifts. The γ-ray spectra were Doppler corrected using the angular information from the AGATA detectors and the velocity vector measured with PRISMA after the ions passed through the degrader. As a consequence, γ rays emitted after the degrader foil appear at the correct transition energy in the spectra, while γ rays emitted before the degrader appear at lower energies when observed at backward angles. The 4.2 mg/cm ^{2} thick Nb degrader was chosen to be thick enough to ensure a sufficient separation between the two components of the γ rays and at the same time thin enough in order to not degrade the mass resolution in PRISMA and to limit the γ count rate from reactions on the degrader to less than 50 kHz per crystal [49].

Data were taken for five distances between the target and degrader foils ranging from 100 to 1900 μm. With typical recoil velocities of $v \approx 30\,\mu$m/ps, the measurement was sensitive to lifetimes ranging from a few to a few tens of picoseconds, which corresponds to the range of lifetimes expected for the $7/2^-$ states of interest. By using event-by-event identification in PRISMA, γ-ray singles spectra were produced for each of the three odd-mass Cu isotopes under study and for each of the five distances. The lifetime of an excited state can be determined from the intensities of the decay transition emitted before and after the degrader, I_f and I_s, respectively, where the indices stand for *fast* and *slow*. The intensities have to be normalized to account for differences in beam intensity and running time during the measurements at different plunger distances. A common way of normalizing intensities taken at different distances is to divide by the sum of both components and obtain the lifetime from the ratio $R = I_s/(I_s + I_f)$. However, in the present case the statistics of the spectra is poor, and it is difficult for some distances to obtain the intensities of both fast and slow components simultaneously. Normalization by the sum of both components

therefore leads to large uncertainties. Higher precision was achieved when the γ-ray intensities were normalized by the number N_A of Cu ions of mass A identified at the focal plane of PRISMA [41,50]. Lifetimes were hence deduced from the ratios $R(d) = I_s(d)/N_A(d)$ at each distance d between the target and stopper foil. The distance d can be related to the flight time t between the foils via $t = d/v$, where v is the velocity before the degrader. This velocity can be obtained from the velocity measured after the degrader with PRISMA and the energy loss of the ions in the degrader. The spectra for the three Cu isotopes under study show no indication of transitions feeding any of the $7/2^-$ states. Under the assumption that the feeding mechanism for these states is fast compared to their decay, the lifetime τ is obtained from the ratio $R(t)$ as $R(t) = \exp(-t/\tau)$. The method was validated by reproducing several known lifetimes in other nuclides (e.g., ^{72}Zn and ^{76}Ge) [41,50].

III. RESULTS

From the present experimental data it was possible to determine the lifetime of the first excited $7/2^-$ state at 1711 keV in ^{69}Cu ($N = 40$) and at 981 keV in ^{71}Cu ($N = 42$) and the third excited $(7/2^-)$ state at 1298 keV in ^{73}Cu ($N = 44$). Doppler-corrected γ-ray spectra were obtained for each Cu isotope after selection in atomic mass number provided by the PRISMA spectrometer (upper panel of Fig. 2). The lower panels of Fig. 2 show the γ-ray transitions, summed over all target-to-degrader distances, from the $7/2^-_1$ to the $3/2^-_1$ ground state for ^{69}Cu and ^{71}Cu, and for the $7/2^-_3$ to the low-lying $5/2^-_1$ state in ^{73}Cu, respectively. Fast and slow components are clearly visible in the spectra. The results for the three isotopes are discussed in detail in the following sections.

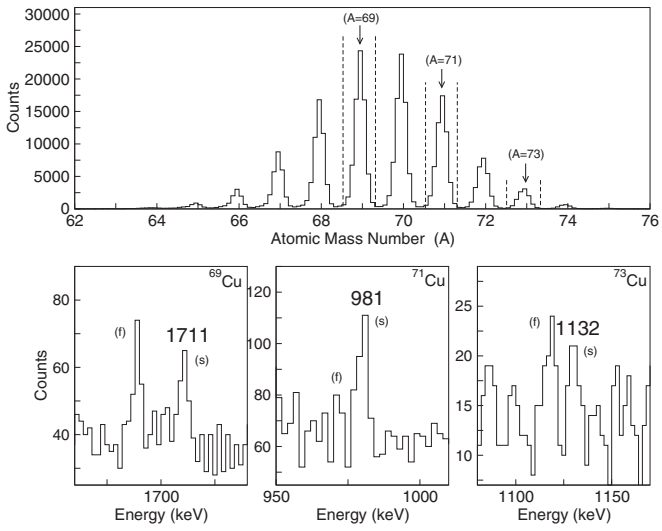

FIG. 2. Mass distribution of Cu isotopes detected in PRISMA, showing the selection of three Cu isotopes (upper panel), and Doppler-corrected γ-ray spectra with fast (f) and slow (s) components for the associated transitions summed over all target-to-degrader distances (lower panel).

A. ^{69}Cu

Knowledge about the energy levels in ^{69}Cu was obtained mainly from β-decay experiments [28,29,51]. The ground-state spin-parity in ^{69}Cu was assigned a $3/2^-$ spin-parity using the technique of collinear laser spectroscopy at ISOLDE [52]. In the β-decay work, a $5/2^-$ and two $7/2^-$ states were identified at excitation energies of 1214, 1711, and 1872 keV, respectively. States with higher excitation energy up to approximately 4 MeV were populated via the deep-inelastic reaction of ^{70}Zn projectiles on a ^{198}Pt target [53]. A $19/2^-$ isomer with a half-life of 22(1) ns was measured in the same work. An early study of the ^{70}Zn$(d,^3$He) reaction provided spectroscopic factors for the first $3/2^-$, $1/2^-$, $5/2^-$, and both $7/2^-$ states [54]. A more recent work extended the measurement of spectroscopic factors to states up to 4 MeV using the same reaction [55].

Collective properties of the low-lying states in ^{69}Cu were studied in a low-energy Coulomb excitation experiment with a radioactive beam [30]. In this experiment $B(E2)$ values were measured for transitions exciting the states at 1096, 1214, and 1872 keV. The $1/2^-$ state at 1096 keV was found to have a similar $B(E2)$ value as in the lighter odd-mass Cu nuclei, while the $5/2^-$ state at 1214 keV was found to have a much lower $B(E2)$ value compared to ^{65,67}Cu, indicating a significant loss of collectivity. The $B(E2)$ value for the excitation of the $7/2^-_2$ state at 1872 keV and its similarity to the $B(E2; 0^+_1 \rightarrow 2^+_1)$ allowed us to identify this state as mainly a $2p_{3/2}$ proton coupled to the even-even ^{68}Ni core. This configuration assignment is supported by the PCM predictions [35]. The fact that the $7/2^-_1$ state was not populated in the Coulomb excitation experiment suggests that its collectivity is low. The PCM calculations predict this state to have a $(\pi 2p_{3/2})^2\, \pi 1f^{-1}_{7/2}$ structure.

The lifetime of the $7/2^-_1$ state at 1711 keV was measured in the present experiment by utilizing the RDDS method. Figure 3 shows the Doppler-corrected γ-ray spectra for five distances ranging from 100 to 1900 μm. The high background level appearing in the spectra (due to the low statistics) was carefully taken into account while determining the intensity of each peak component. Since no feeding transitions were observed in the γ-ray spectra for the state of interest, the intensity ratio $R(t)$ was fitted with an exponential function as described above. Figure 4 shows the result of the fit for the 1711-keV $7/2^-_1 \rightarrow 3/2^-_1$ transition. The lifetime of the $7/2^-_1$ state at 1711 keV was found to be 37(16) ps, corresponding to the reduced transition rate $B(E2; 7/2^-_1 \rightarrow 3/2^-_1) = 1.5(6)\ e^2\,\mathrm{fm}^4$.

B. ^{71}Cu

The ground state of ^{71}Cu was found to have spin-parity $3/2^-$ [32,52]. The most detailed experimental knowledge on excited states, with attempted spin assignments, originate from the β-decay work of Franchoo *et al.* [28,29]. Spin-parity $5/2^-$ was assigned to the state at 534 keV excitation energy, and $7/2^-$ to both states at 981 and 1190 keV, respectively. An experiment using deep-inelastic reactions of a ^{64}Ni beam on a thick ^{238}U target has extended the level scheme up to around 5.3 MeV, including an isomeric $19/2^-$ state [31]. A recent

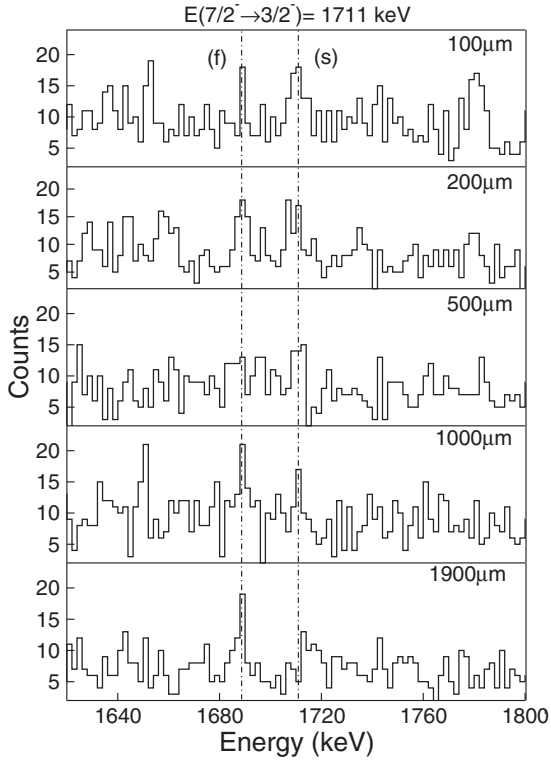

FIG. 3. Doppler-corrected γ-ray spectra for ^{69}Cu. The positions of the fast (f) and slow (s) components of the 1711-keV $7/2^-_1 \rightarrow 3/2^-_1$ transition are indicated by the dashed lines.

study of the ^{72}Zn$(d,^3$He$)^{71}$Cu reaction provided spectroscopic factors for the first $3/2^-$ and $5/2^-$ and three low-lying $7/2^-$ states in ^{71}Cu [56,57].

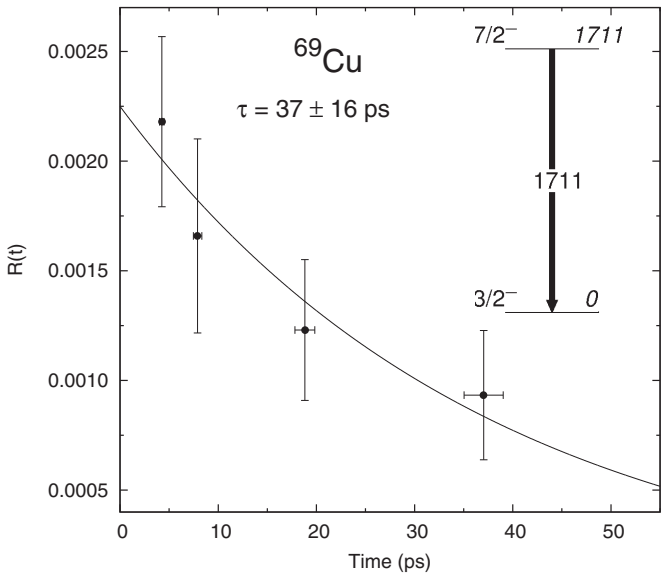

FIG. 4. Experimental $R(t)$ values as a function of the flight time between the target and degrader foils for the $7/2^-_1 \rightarrow 3/2^-_1$ state in ^{69}Cu and the result of the exponential fit. The data point corresponding to the distance at 1900 μm is excluded in the lifetime analysis.

The collectivity of the low-lying states was studied in the Coulomb excitation experiment of Stefanescu *et al.* [30], where $B(E2)$ values were determined for the transitions de-exciting the $1/2^-_1$, $5/2^-_1$, and $7/2^-_2$ states. The newly identified $1/2^-_1$ state at 454 keV with its large $B(E2)$ value of more than 20 Weisskopf units was found to be collective rather than being of single-particle character based on the $\pi 2p_{1/2}$ configuration. The single-particle character of the $5/2^-_1$ state at 534 keV has been understood from the sudden decrease of the $B(E2)$ value with respect to those in the lighter Cu isotopes. Similar to the case of ^{69}Cu, the $7/2^-_2$ state at 1190 keV was interpreted as a $2p_{3/2}$ proton coupled to the 2^+_1 state in the ^{70}Ni core based on the similarity of the respective $B(E2)$ values. Again, this assignment is supported by PCM calculations [35]. The $7/2^-_1$ state at 981 keV was tentatively assigned as a 2p-1h excitation in both the β-decay study [29] and the PCM calculations [35].

In the present work the $B(E2; 7/2^-_1 \rightarrow 3/2^-_1)$ value was determined by measuring the lifetime of the $7/2^-_1$ state. Preliminary results on this state were previously reported in Ref. [58]. Figure 5 shows the Doppler-corrected γ-ray spectra obtained for four distances up to 1000 μm. The spectrum measured at a distance of 1900 μm was not used in the analysis as it lies outside the sensitive region for the measured lifetime. Again, no transitions feeding the $7/2^-_1$ state could be identified. Figure 6 shows the $R(t)$ ratio and the result of the

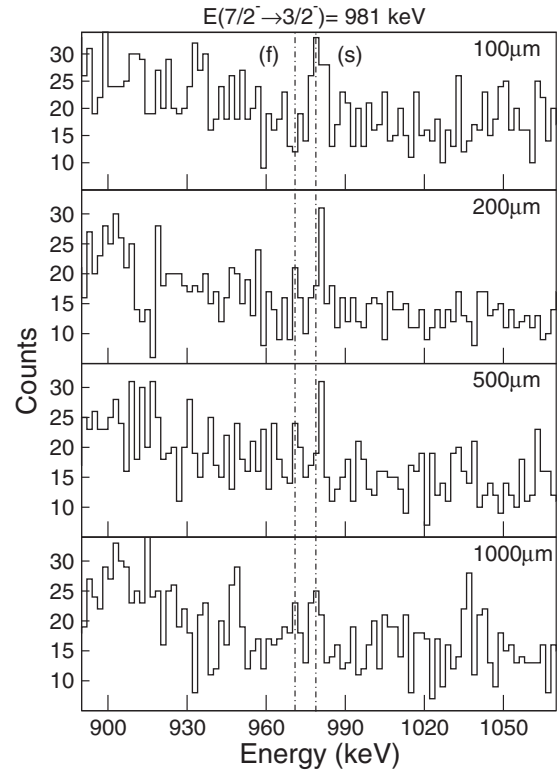

FIG. 5. Doppler-corrected γ-ray spectra for ^{71}Cu. The positions of the fast (f) and slow (s) components of the 981-keV $7/2^-_1 \rightarrow 3/2^-_1$ transition are indicated by the dashed lines.

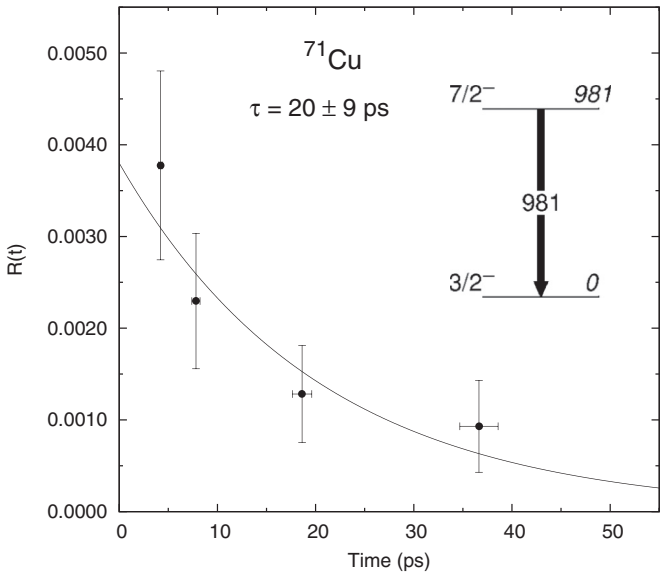

FIG. 6. Experimental $R(t)$ values for the $B(E2; 7/2_1^- \rightarrow 3/2_1^-)$ transition in ^{71}Cu as a function of the flight time between the target and degrader foil, and the result of the exponential fit.

exponential fit. A lifetime value of $\tau = 20(9)$ ps was extracted; this corresponds to $B(E2; 7/2_1^- \rightarrow 3/2_1^- = 44(20)\ e^2\,\mathrm{fm}^4$.

C. ^{73}Cu

The spin and parity of the ground state of ^{73}Cu were measured by laser spectroscopy to be $3/2^-$ [32,52]. Further experimental information on excited states in ^{73}Cu comes from β-decay and Coulomb excitation experiments [28–30]. The low-lying excited states at 166 keV was assigned as $5/2^-$, whereas the three states at 961, 1010, and 1298 keV were all tentatively assigned as $7/2^-$ states in the β-decay measurement [28,29]. A further low-lying state was identified at 135 keV and assigned spin-parity $1/2^-$ in the Coulomb excitation experiment, which also yielded the $B(E2)$ values for the excitations to the $1/2_1^-$, $5/2_1^-$, and $7/2_1^-$ states [30]. The $1/2_1^-$ state at 135 keV was found to be collective on the basis of its large $B(E2; 1/2_1^- \rightarrow 3/2_1^-)$ value of 23.1(21) Weisskopf units. The $5/2_1^-$ state, on the other hand, was found to have single-particle character with a $B(E2; 5/2_1^- \rightarrow 3/2_1^-)$ value of 4.4(5) Weisskopf units. The $B(E2; 7/2_1^- \rightarrow 3/2_1^-)$ value follows the trend of the $B(E2; 2_1^+ \rightarrow 0_1^+)$ values in the even-even Ni isotopes, and the $7/2_1^-$ state at 961 keV was interpreted as a particle-core coupled state, in agreement with predictions from the PCM calculations [35]. The other two $7/2^-$ states at 1010 and 1298 keV, which were not populated in the Coulomb excitation experiment, were interpreted as 2p-1h and $\pi 1 f_{5/2} \otimes 2_1^+$ (^{72}Ni) states, respectively, in the β-decay study [29].

In the present experiment, it was possible to extract the lifetime of the $(7/2_3^-)$ state at 1298 keV. Figure 7 shows the Doppler-corrected γ-ray spectra for the relevant energy region. The peak at 1132 keV and its shifted component are visible in each spectrum corresponding to different distances between target and degrader. The longest distance of 1900 μm was not included in the lifetime analysis because it lies outside the region of sensitivity. Figure 8 shows the $R(t)$ ratios as a function of the flight time between the target and degrader foils together with an exponential fit, which yielded a lifetime

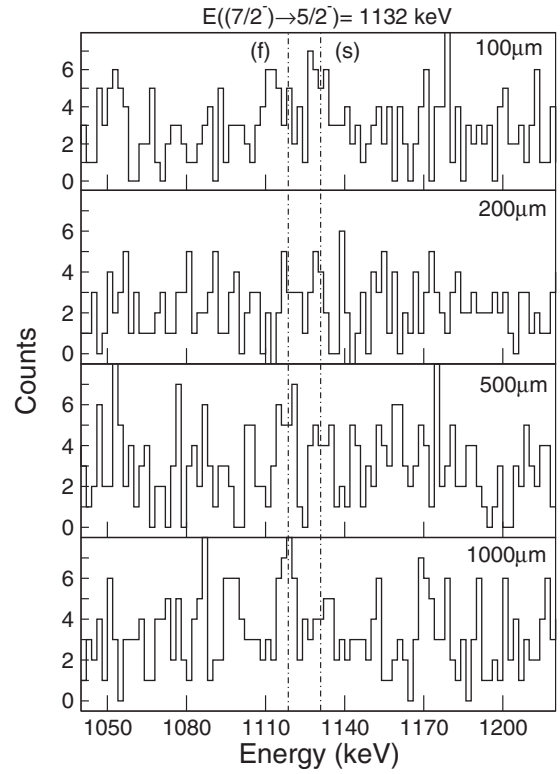

FIG. 7. Doppler-corrected γ-ray spectra for ^{73}Cu. The positions of the fast (f) and slow (s) components of the 1132-keV $7/2_3^- \rightarrow 5/2_1^-$ transition are indicated by the dashed lines.

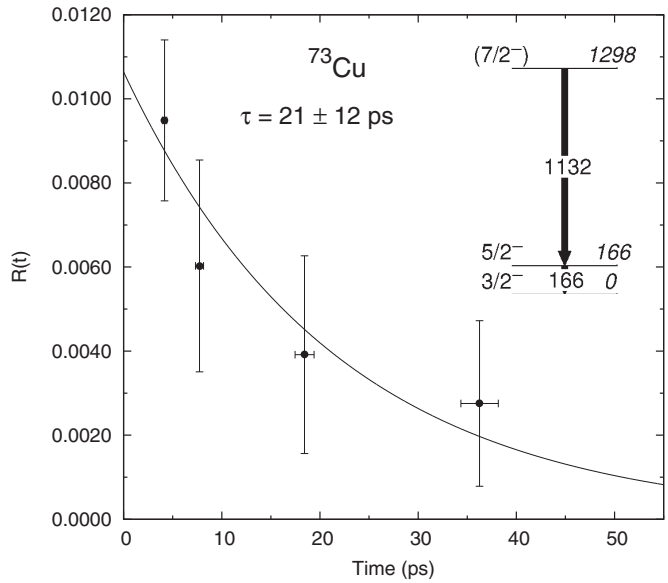

FIG. 8. Experimental $R(t)$ values for the $B(E2; (7/2_3^-) \rightarrow 5/2_1^-)$ transition in ^{73}Cu as a function of the flight time between the target and degrader foil, and the result of the exponential fit.

TABLE I. Experimental lifetime values for states in ^{69,71,73}Cu and resulting $B(E2)$ transition probabilities.

Nucleus	$J_i^\pi \rightarrow J_f^\pi$	E_{level} (keV)	τ (ps)	E_γ (keV)	$B(E2)$ (e^2 fm^4)
^{69}Cu	$7/2_1^- \rightarrow 3/2_1^-$	1711	37(16)	1711	1.5(6)
^{71}Cu	$7/2_1^- \rightarrow 3/2_1^-$	981	20(9)	981	44(20)
^{73}Cu	$(7/2_3^-) \rightarrow 5/2_1^-$	1298	21(12)	1132	20(11)

value of $\tau = 21(12)$ ps. By assuming that the transition has $E2$ character, the measured lifetime corresponds to $B(E2; 7/2_3^- \rightarrow 5/2_1^-) = 20(11)\ e^2\,\text{fm}^4$. Table I summarizes the lifetimes and $B(E2)$ values obtained in the present work for ^{69,71,73}Cu.

IV. DISCUSSION

Transition probabilities obtained in the present work are compared with state-of-the-art LSSM calculations in Table II. The calculations were carried out using a model space comprising the pf shell for protons and the $2p_{3/2}$, $2p_{1/2}$, $1f_{5/2}$, $1g_{9/2}$, and $2d_{5/2}$ orbitals for neutrons. Due to the large dimension of the configuration space, truncations of 9p-9h for ^{69}Cu and 8p-8h for ^{71,73}Cu across the $Z = 28$ and $N = 40$ shell gaps were applied in the calculations.

The LNPS effective interaction with minor revisions was used in the calculations. It combines two-body matrix elements based on the KB3gr interaction for the pf shell, a renormalized G-matrix interaction for the $2p_{3/2}$, $2p_{1/2}$, $1f_{5/2}$, and $1g_{9/2}$ neutron orbitals, and a G-matrix interaction based on the Kahana-Lee-Scott potential for the remaining neutron $2d_{5/2}$ orbital [26,59]. The calculations were performed using the shell-model codes ANTOINE and NATHAN [60,61]. Standard effective charges of $e_\pi = 1.5e$ and $e_\nu = 0.5e$ for protons and neutrons, respectively, were used to obtain the $B(E2)$ transition rates.

TABLE II. $B(E2)$ transition rates obtained in shell-model calculations compared to experimental results from Coulomb excitation [30] and the present lifetime measurement. Experimental $B(E2)$ values obtained in the present work are indicated with a box.

$J_f^\pi \rightarrow J_i^\pi$	$E_{\text{level}}^{\text{exp}}$ (keV)	$E_{\text{level}}^{\text{theor}}$ (keV)	E_γ^{exp} (keV)	E_γ^{theor} (keV)	$B(E2)^{\text{exp}}$ (e^2 fm^4)	$B(E2)^{\text{theor}}$ (e^2 fm^4)
^{69}Cu						
$5/2_1^- \rightarrow 3/2_1^-$	1214	1249	1214	1249	50(8)	28.5
$7/2_1^- \rightarrow 3/2_1^-$	1711	2186	1711	2186	1.5(6)	0.05
$7/2_2^- \rightarrow 3/2_1^-$	1872	1862	1872	1862	77(12)	46
^{71}Cu						
$5/2_1^- \rightarrow 3/2_1^-$	534	276	534	276	68(8.8)	54
$7/2_1^- \rightarrow 3/2_1^-$	981	1426	981	1426	44(20)	14.4
$7/2_2^- \rightarrow 3/2_1^-$	1189	1115	1189	1115	187(2)	179
^{73}Cu						
$5/2_1^- \rightarrow 3/2_1^-$	166	0	166	−62	80(9)	65
$7/2_1^- \rightarrow 3/2_1^-$	961	937	961	875	270(3)	251
$7/2_3^- \rightarrow 5/2_1^-$	1298	1128	1132	1128	20(11)	0.02
$5/2_2^- \rightarrow 5/2_1^-$	1298	1203	1132	1203	20(11)	11.4

A. ^{69}Cu

The shell-model calculations predict the ground state to have spin and parity $3/2^-$ with a dominant $\pi 2p_{3/2}$ component in the wave function. The lowest $5/2^-$ state is based mainly on the $\pi 1f_{5/2}$ configuration and is found at 1249 keV, compared with the experimental excitation energy of 1214 keV. The calculated $B(E2)$ value of 28.5 $e^2\,\text{fm}^4$ is in reasonable agreement with the experimental value of 50(8) $e^2\,\text{fm}^4$. Two low-lying states with spin and parity $7/2^-$ are found at 1862 and 2186 keV in the calculations. The lower one at 1862 keV has a dominant component of the wave function (40%) originating from one particle in the $\pi 2p_{3/2}$ orbital coupled to the neutron 2_1^+ state in the ^{68}Ni core, i.e., $\pi 2p_{3/2} \otimes 2_1^+$ (^{68}Ni). The transition rate from this state was calculated to be $B(E2; 7/2^- \rightarrow 3/2^-) = 46\ e^2\,\text{fm}^4$, compared with the experimental value of 77(12) $e^2\,\text{fm}^4$ from the Coulomb excitation measurement [30]. The calculated $7/2_1^-$ state can hence be associated with the experimental $7/2_2^-$ state, and the calculations support the previous interpretation of the state. The second calculated $7/2^-$ state at 2186 keV has a very small transition rate to the ground state, $B(E2; 7/2^- \rightarrow 3/2^-) = 0.05\ e^2\,\text{fm}^4$, and can therefore be associated with the $7/2_1^-$ state at 1711 keV, for which the transition rate was found to be small. It has a considerable $\pi 1f_{5/2} \otimes 2_1^+$ (^{68}Ni) contribution with 52% of the wave function amplitude. Both $7/2^-$ states carry a low spectroscopic factor in the calculations and their pure $\pi 1f_{7/2}$ hole component is 12% and 16%, respectively. However, experimental spectroscopic factors in Ref. [55] demonstrate that the present calculations underestimate the low-lying strength in ^{69}Cu.

B. ^{71}Cu

Also in the case of ^{71}Cu, both the $3/2^-$ ground state and the first excited $5/2^-$ state are well reproduced in the calculations with a dominant proton $\pi 2p_{3/2}$ and $\pi 1f_{5/2}$ component in the wave function, respectively. The shell-model value of $B(E2; 5/2^- \rightarrow 3/2^-) = 54\ e^2\,\text{fm}^4$ is in good agreement with the experimental value from Coulomb excitation [30].

Among the two excited $7/2^-$ states found in the shell-model calculation, the one at 1115 keV excitation energy has a strong $B(E2)$ strength to the ground state and can be associated with the $7/2_2^-$ state at 1189 keV, which was found to be collective in the Coulomb excitation measurement [30]. Its wave function is dominated by the $\pi 2p_{3/2} \otimes 2_1^+$(^{70}Ni) configuration with an amplitude of 59%. The calculated $7/2^-$ state at 1426 keV could be associated with the $7/2_1^-$ state at 981 keV, although it lies too high in the present calculations. The calculated $B(E2)$ value is strongly quenched compared to the experimental value found in the present work, as a result of its structure being dominated by the $\pi 1f_{5/2} \otimes 2_1^+$ (^{70}Ni) coupling (55%). The larger experimental $B(E2)$ value excludes single-hole character, which was previously suggested for this state [29,35].

In a recent study of the single-particle strength in ^{71}Cu via the $(d,{}^3\text{He})$ reaction, no $f_{7/2}$ strength was observed around 1 MeV [56,57]. This suggests that neither of the two experimentally observed states arises from a single proton-hole excitation. This is consistent with the present shell-model

calculation predicting other components to dominate the wave functions of the lowest $7/2^-$ states in this nucleus.

C. ^{73}Cu

The shell-model calculations find the $5/2^-$ state to be the ground state in ^{73}Cu with an excited $3/2^-$ state at 62 keV, whereas experimentally the $5/2^-$ state is found at 166 keV excitation above the $3/2^-$ ground state, and the inversion of the $\pi 1f_{5/2}$ and $\pi 2p_{3/2}$ single-particle states occurs only in ^{75}Cu. Two close-lying $7/2^-$ states are predicted at 875 and 1066 keV above the $3/2^-$ state, respectively. In the calculation the first $7/2^-$ state is connected via a strong $E2$ transition to the $3/2^-$ state, with a $B(E2)$ value very close to the experimental one known from the Coulomb excitation measurement [30]. The wave function of this state is dominated by the $\pi 2p_{3/2} \otimes 2_1^+(^{72}\text{Ni})$ coupling with an amplitude of 45%. The $B(E2)$ values from the second $7/2^-$ state at 1128 keV to both the $5/2^-$ and $3/2^-$ states are calculated to be nearly zero. Contrary to the case of ^{69,71}Cu, this state has a single-hole character, with 6.4 particles in the proton $f_{7/2}$ orbital. Indeed, the energy decrease of the proton-hole state in ^{73}Cu is expected as the $Z = 28$ shell gap is reduced and the $\pi 1f_{5/2}$ orbit is lowered by the increasing neutron occupancy of the $\nu 1g_{9/2}$ orbital between $N = 40$ and $N = 50$. One-proton separation energies from the present shell-model calculations can be used to estimate the shell gap to be 4.5 MeV at $N = 44$, compared to an experimental value of 5.1 MeV [62]. This somewhat smaller shell gap is consistent with the fact that the model predicts the inversion of the $\pi 1f_{5/2}$ and $\pi 2p_{3/2}$ single-particle states already for ^{73}Cu instead of ^{75}Cu. The calculated $Z = 28$ shell gap of 5.3 MeV at $N = 42$ is in good agreement with the experimental value of 5.5 MeV and explains the absence of a proton-hole $7/2^-$ state at very low energy in ^{71}Cu.

Since the spin-parity of the state at 1298 keV is only tentatively assigned as $7/2^-$ in the previous experimental studies [28,29], we considered different spin assignments for this state in the current shell-model calculations. The lowest $9/2^-$ state is found at an excitation energy of 970 keV, which is not too far from the experimental value. However, the $9/2^-$ state is connected by a large $B(E2)$ strength to the $5/2^-$ state, which is incompatible with the experimental $B(E2)$ value. Better agreement is obtained for a spin and parity assignment of a second $5/2^-$ state. Its excitation energy is calculated to be 1203 keV, and the $B(E2)$ strength to the first $5/2^-$ state is within a factor of 2 compared to the experimental value (see Table II). The underestimation of the predicted $B(E2)$ value can be due to the missing $M1$ magnetic dipole component, which is expected to be pronounced for a transition between two levels with the same spin and parity. The wave functions of the second $5/2^-$ state are rather mixed and mainly coming from one proton in the $\pi 1f_{5/2}$ orbital coupled to the 0_1^+ state in ^{72}Ni (23%) and one proton in the $\pi 1f_{5/2}$ orbital coupled to the 2_1^+ state in ^{72}Ni (22%).

V. CONCLUSION

Three low-lying $7/2^-$ states can emerge in neutron-rich Cu isotopes from single-proton excitations above the $Z = 28$ gap or from the coupling of a proton in the $\pi 2p_{3/2}$ or $\pi 1f_{5/2}$ orbital to the 2_1^+ state of the even-even Ni core. In order to understand the underlying structure of the various $7/2^-$ states, $B(E2)$ transition probabilities in ^{69,71,73}Cu were determined through lifetime measurements using the RDDS method. The Cu nuclei populated after multinucleon transfer reactions were identified by the PRISMA magnetic spectrometer while the emitted γ rays were detected in the AGATA Demonstrator. A comparison of the transition probabilities to shell-model calculations shows that the different possible configurations lie close in energy and that the wave functions of the lowest $7/2^-$ state can be rather mixed. The position and collective nature of those $7/2^-$ states in ^{69,71,73}Cu that were interpreted as one proton in the $2p_{3/2}$ orbital coupled to the 2_1^+ core [30] were reproduced with good agreement by the calculations. The $7/2_1^-$ states in ^{69,71}Cu at 1711 and 981 keV, respectively, were found to have a significant contribution from the $\pi 1f_{5/2} \otimes 2_1^+$ (^{68,70}Ni) structure. However, the calculated excitation energies for these states are systematically too high. Only the $(7/2^-)$ state at 1298 keV in ^{73}Cu could potentially be explained as a 2p-1h excitation across the proton shell gap. The absence of a low-lying proton-hole state at $N = 40$ and 42 in the present shell-model calculations is consistent with a reduction of the $Z = 28$ gap toward 50. However, the state at 1298 keV in ^{73}Cu and its transition strength could also be explained as a second $5/2^-$ state with reasonable agreement between the shell-model calculations and experimental values. Further experimental and theoretical studies are needed to clarify the low-energy structure in Cu nuclei with increasing number of neutrons in the $\nu 1g_{9/2}$ orbital.

ACKNOWLEDGMENTS

This work has been partially supported by the European Union Seventh Framework Program FP7/2007-2013 under Grant Agreement No. 262010, ENSAR and MINECO, Spain, under Grants No. FPA2011-29854-C03 and No. FPA2011-29854-C04, Generalitat Valenciana, Spain, under Grant No. PROMETEOII/2014/019, and MINECO, Spain, under Grant Consolider-Ingenio 2010 CSD2007-00042.

[1] M. Goeppert-Mayer, Phys. Rev. **74**, 235 (1948).
[2] I. Hamamoto, S. V. Lukyanov, and X. Z. Zhang, Nucl. Phys. A **683**, 255 (2001).
[3] T. Otsuka *et al.*, Prog. Theor. Phys. Suppl. **146**, 6 (2002).
[4] T. Otsuka, T. Suzuki, R. Fujimoto, H. Grawe, and Y. Akaishi, Phys. Rev. Lett. **95**, 232502 (2005), and references therein.
[5] T. Otsuka, T. Suzuki, R. Fujimoto, T. Matsuo, D. Abe, H. Grawe, and Y. Akaishi, Acta Phys. Pol. B **36**, 1213 (2005).

[6] O. Sorlin and M.-G. Porquet, Prog. Part. Nucl. Phys. **61**, 602 (2008).
[7] T. Otsuka, T. Suzuki, M. Honma, Y. Utsuno, N. Tsunoda, K. Tsukiyama, and M. Hjorth-Jensen, Phys. Rev. Lett. **104**, 012501 (2010).
[8] N. A. Smirnova, K. Heyde, B. Bally, F. Nowacki, and K. Sieja, Phys. Lett. B **686**, 109 (2010).
[9] N. A. Smirnova, K. Heyde, B. Bally, F. Nowacki, and K. Sieja, Phys. Rev. C **86**, 034314 (2012).
[10] T. Otsuka, Phys. Scr. T **152**, 014007 (2013).
[11] Y. Utsuno, T. Otsuka, N. Shimizu, M. Honma, T. Mizusaki, Y. Tsunoda, and T. Abe, EPJ Web Conf. **66**, 02106 (2014).
[12] M. Belleguic *et al.*, Nucl. Phys. A **682**, 136c (2001).
[13] E. Becheva *et al.*, Phys. Rev. Lett. **96**, 012501 (2006).
[14] R. Kanungo *et al.*, Phys. Rev. Lett. **102**, 152501 (2009).
[15] C. R. Hoffman *et al.*, Phys. Lett. B **672**, 17 (2009).
[16] A. Huck *et al.*, Phys. Rev. C **31**, 2226 (1985).
[17] A. Gade *et al.*, Phys. Rev. C **74**, 021302(R) (2006).
[18] D. Guillemaud-Mueller *et al.*, Nucl. Phys. A **426**, 37 (1984).
[19] T. Motobayashi *et al.*, Phys. Lett. B **346**, 9 (1995).
[20] J. Fridman *et al.*, Nature (London) **435**, 922 (2005).
[21] B. Bastin *et al.*, Phys. Rev. Lett. **99**, 022503 (2007).
[22] D. Steppenbeck *et al.*, Nature (London) **502**, 207 (2013).
[23] D. Steppenbeck *et al.*, J. Phys.: Conf. Ser. **445**, 012012 (2013).
[24] M. Honma, T. Otsuka, T. Mizusaki, and M. Hjorth-Jensen, Phys. Rev. C **80**, 064323 (2009).
[25] K. Sieja and F. Nowacki, Phys. Rev. C **81**, 061303(R) (2010).
[26] K. Sieja and F. Nowacki, Phys. Rev. C **85**, 051301(R) (2012).
[27] T. Otsuka, T. Matsuo, and D. Abe, Phys. Rev. Lett. **97**, 162501 (2006).
[28] S. Franchoo *et al.*, Phys. Rev. Lett. **81**, 3100 (1998).
[29] S. Franchoo *et al.*, Phys. Rev. C **64**, 054308 (2001).
[30] I. Stefanescu *et al.*, Phys. Rev. Lett. **100**, 112502 (2008).
[31] I. Stefanescu *et al.*, Phys. Rev. C **79**, 034319 (2009).
[32] K. T. Flanagan *et al.*, Phys. Rev. Lett. **103**, 142501 (2009).
[33] G. Bocchi *et al.*, Phys. Rev. C **89**, 054302 (2014).
[34] C. R. Niţă *et al.*, Phys. Rev. C **89**, 064314 (2014).
[35] A. M. Oros-Peusquens and P. F. Mantica, Nucl. Phys. A **669**, 217c (2000).
[36] A. Gadea *et al.*, Nucl. Instrum. Methods A **654**, 88 (2011).
[37] S. Akkoyunlu *et al.*, Nucl. Instrum. Methods A **668**, 26 (2012).
[38] A. M. Stefanini *et al.*, Nucl. Phys. A **701**, 217c (2002).
[39] G. Montagnoli *et al.*, Nucl. Instrum. Methods A **547**, 455 (2005).
[40] S. Beghini *et al.*, Nucl. Instrum. Methods A **551**, 364 (2005).
[41] M. Doncel, Ph.D. thesis, University of Salamanca, Spain, 2012.
[42] R. Venturelli and D. Bazzacco, LNL Annual Report (2004), INFN-LNL, Legnaro, Italy, p. 220, 2005.
[43] A. Lopez-Martens *et al.*, Nucl. Instrum. Methods Phys. Res., Sect. A **533**, 454 (2004).
[44] D. Bazzacco, Nucl. Phys. A **746**, 248c (2004).
[45] J. J. Valiente-Dobon *et al.*, Phys. Rev. Lett. **102**, 242502 (2009).
[46] D. Mengoni *et al.*, Eur. Phys. J. A **42**, 387 (2009).
[47] D. Mengoni *et al.*, Phys. Rev. C **82**, 024308 (2010).
[48] A. Dewald, O. Möller, and P. Petkov, Prog. Part. Nucl. Phys. **67**, 786 (2012).
[49] A. Goasduff *et al.*, Nucl. Instrum. Methods A **758**, 1 (2014).
[50] M. Doncel *et al.* [Eur. Phys. J. A (to be submitted)].
[51] U. Bosch, W.-D. Schmidt-Ott, E. Runte, P. Tidemand-Petersson, P. Koschel, and F. Meissner, Nucl. Phys. A **477**, 89 (1988).
[52] P. Vingerhoets *et al.*, Phys. Rev. C **82**, 064311 (2010).
[53] T. Ishii, M. Asai, A. Makishima, I. Hossain, M. Ogawa, J. Hasegawa, M. Matsuda, and S. Ichikawa, Phys. Rev. Lett. **84**, 39 (2000).
[54] B. Zeidman and J. A. Nolen, Phys. Rev. C **18**, 2122 (1978).
[55] P. Morfouace *et al.*, Acta Phys. Pol. B **45**, 243 (2014).
[56] S. Franchoo *et al.* (private communication).
[57] P. Morfouace, Ph.D. thesis, Institut de Physique Nucléaire, Orsay, France, 2014.
[58] M. Doncel *et al.*, Acta Phys. Pol. B **44**, 505 (2013).
[59] S. M. Lenzi, F. Nowacki, A. Poves, and K. Sieja, Phys. Rev. C **82**, 054301 (2010).
[60] E. Caurier, G. Martinez-Pinedo, F. Nowacki, A. Poves, and A. P. Zuker, Rev. Mod. Phys. **77**, 427 (2005).
[61] E. Caurier and F. Nowacki, Acta Phys. Pol. B **30**, 705 (1999).
[62] M. Wang, G. Audi, A. H. Wapstra, F. G. Kondev, M. MacCormick, X. Xu, and B. Pfeiffer, Chin. Phys. C **36**, 1603 (2012).